# INJECTION EFFICIENCY MONITORING SYSTEM AT THE AUSTRALIAN SYNCHROTRON

E. van Garderen, M. Boland, S. Griffiths, G. LeBlanc, S. Murphy, A. Rhyder, A. Starritt,
Australian Synchrotron, Clayton, Victoria, Australia

## *Abstract*

The Australian Synchrotron upgraded its user mode from decay mode to top-up mode in May 2012. To monitor the beam charge passing through the accelerator systems at key transfer points the transmission efficiency system has been upgraded. The original system could only measure the efficiency of the booster to storage ring injection. The new one calculates intermediate efficiencies between six points along the injection system, from the electron gun to the booster-to-storage ring transfer line. This is helpful to diagnose in real-time shot-to-shot the performance of the pulsed magnets, ramped magnets and ramped RF systems and their associated triggers. A software-based injection efficiency interlock has also been introduced, that can inhibit the gun when the machine settings are not optimal. This article details the architecture of the injection efficiency system and lists the improvements on the machine that have been carried out to obtain high quality data.

## INTRODUCTION

The Australian synchrotron is a 3 GeV machine that ran in decay mode until May 2012, with two daily injections to 200 mA. Top-up operations were then introduced as default user mode. Because of the stringent beam performance requirements for top-up better diagnostics equipment was needed. This was especially the case of the injection efficiency as transmission along the machine needed to be identified and monitored in order to optimise the top-up procedure.

The injection efficiency system that was originally installed included only two Direct Current-Current Transformers (DCCTs), in the booster (BO) and in the storage ring (SR). A new system has been built that uses five fast current transformers (FCTs): two in the linac-to-booster transfer line (LTB), one in the first quarter of the booster and two in the booster-to-storage ring transfer line (BTS). In addition to the FCTs the wall current monitor (WCM) located just behind the electron gun also became part of the new injection efficiency monitoring system.

The injection efficiency monitoring is real-time. A software interlock could therefore be introduced that prevents the gun from firing in case its value is too low.

This article is a follow up of [1]. A description of the monitoring devices can be found in [2].

## THE ORIGINAL SYSTEM

The original injection efficiency system uses only two monitors: two DCCTs, one in the booster ring and one in the Storage Ring.

The analogue reading the DCCTs are processed by electronic cards from Bergoz and converted to digital data by two PCI 6281 analogue-to-digital converters (ADCs) from National Instrument. Figure 1 shows the schematics of the original injection efficiency system.

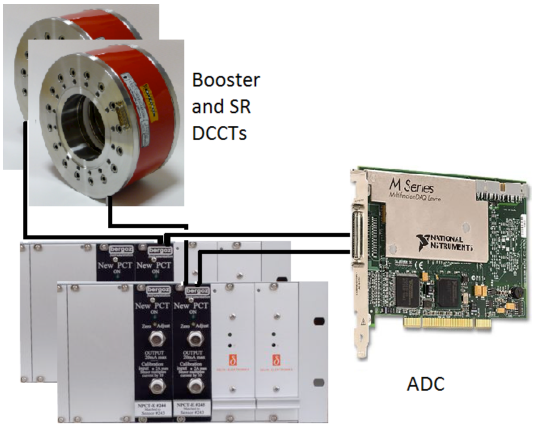

Figure 1: Schematics of the original injection efficiency system.

Both DCCTs measure the current for 50 ms. The signals from the two DCCTs are acquired 300 ms after the gun is fired. The signal from the SR DCCT is acquired once more 450 ms later. As the extraction from the booster happens 602 ms after the gun is fired, 300 ms corresponds to half the booster ramp.

Because the base current in the SR is not null, one needs to calculate the injected current, or delta current, by subtracting the SR DCCT's readings before and after injection.

The signals of the two DCCTs are sent to a input-output controller (IOC) which performs the injection efficiency $IE$ calculation, where $I$ stands for the beam intensity and $L$ for the length of the ring:

$$IE = (\Delta I_{SR} * L_{SR})/(I_{BO} * L_{BO}).$$

At the Australian Synchrotron the length of the Booster $L_{BO}$ is 130.2 m and the length of the Storage Ring $L_{SR}$ is 216 m.

The IOC's driver is EPICS-based to comply with the control system in place at the Australian Synchrotron. All

EPICS data are provided as process variables (PVs) and can be accessed from any computer on the network.

Before top-up was introduced the injection efficiency value from the DCCTs had been used to optimise the BO magnet settings. The common value during decay mode was 85%.

## THE NEW SYSTEM

The new system uses the signals from the WCM and the five FCTs located along the machine (2 in the LTB, 1 in the BO and 2 in the BTS). The data acquisition is performed by three Acqiris U1071A ADC cards from Agilent located in an IOC. The driver is EPICS-based.

The ADCs have a 200 MHz bandwidth although the radio-frequency of the machine is 499.65 MHz. Our system does therefore not allow to distinguish between each electron bunch. Nevertheless this situation is overcome by calibration (see further). The ADCs return the envelope of the signal which is sufficient for our measurement. Figure 2 shows the consequences of using a low bandwidth ADC on a high resolution signal.

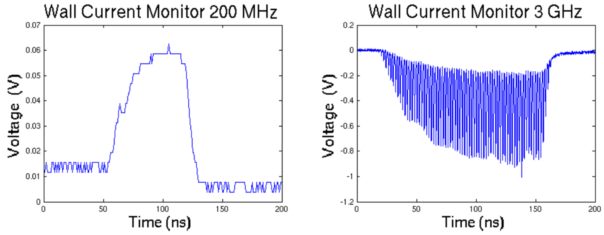

Figure 2: WCM data acquired at 200 MHz (left) and a 3 GHz (right).

The ADCs are triggered by the 1 Hz injection and extraction events, generated by the event generator and delivered to the cards via an event receiver (EVR), part of our timing system [3]. The WCM and FCTs from the LTB are triggered by the injection trigger while FCTs from the BTS are triggered by the extraction trigger. The trigger of the BO FCT is a logical OR of both events as this monitor should provide data at both injection and extraction.

Figure 3 shows the electrical diagram of the new injection efficiency monitoring system.

### *Software Calculation and Calibration*

As explained above the ADCs return signals that are the envelopes of the bunch train, which normally contains 75 bunches. The data are saved as EPICS process variable arrays with 500 points each. The software performs a peak detection, measures the signal height and the position of the base line. It discards the lower 10% of the signal in order to reduce uncertainties associated with the peak detection.

The data is then calibrated. For each monitor, the charge $Q$ in pC is proportional to the integrated signal $I$ in V.s:

$Q = I/a$

where $a$ is a calibration factor expressed in V.s/C.

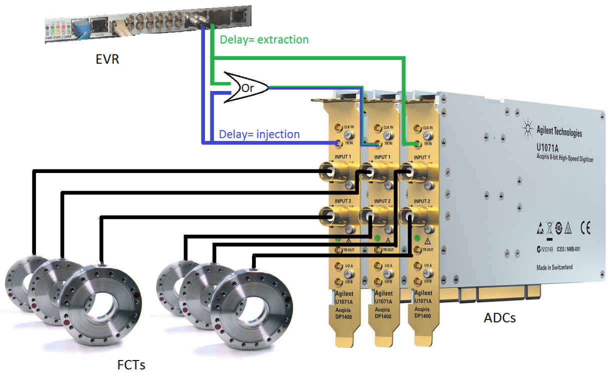

Figure 3: Schematics of the new injection efficiency monitoring system showing the current monitors, the data acquisition cards and the triggering system.

The systematic error due to the bandwidth limiting the bunch train signal is cancelled out by taking the ratio of the signal from two monitors. Using this method the absolute bunch charge in pC does not need to be measured for each monitor as we are only interested in the transmission efficiency. The main source of signal attenuation that has to be compensated for is due to the cables. The calibration factor has thus been determined experientially, as follows:

To calibrate the WCM and FCTs' readings the cable attenuations were measured using a DG535 delay generator from Stanford Research Systems. A DG535 was set to generate a 1 V, 50 ns, square pulse. A first set of measurements was taken by connecting the DG535 directly to the acquisition card outside the machine and a second set by connecting the DG535 inside the machine at the end of the FCTs signal cables. The calibration factor $a$ was calculated as the ratio of the two signals.

### *Noise Reduction*

A few FCT signals were very noisy, especially those from the BTS. To increase their signal-to-noise ratio improvements have been made on the shielding of the extraction septa and kicker.

**Septa** Large currents were induced into the vacuum vessel and earthing system by the extraction septum and pre-septum which could be observed on the monitors located both downstream and upstream of the septa. As there was no direct return path for these currents, peak currents over 30 A were created through the local earthing cables. To improve the design a copper braid was connected to the vacuum vessel, at both ends of each septum, to the aluminium yoke support of the extraction septa. The yoke support provided a low impedance path for the induced current to flow. This reduced the intensity of the induced current seen on the various FCTs by up to 75 %, as shown in Figure 4.

**Kicker** Similarly, the extraction kicker return current was observed to flow through the earthing system and the

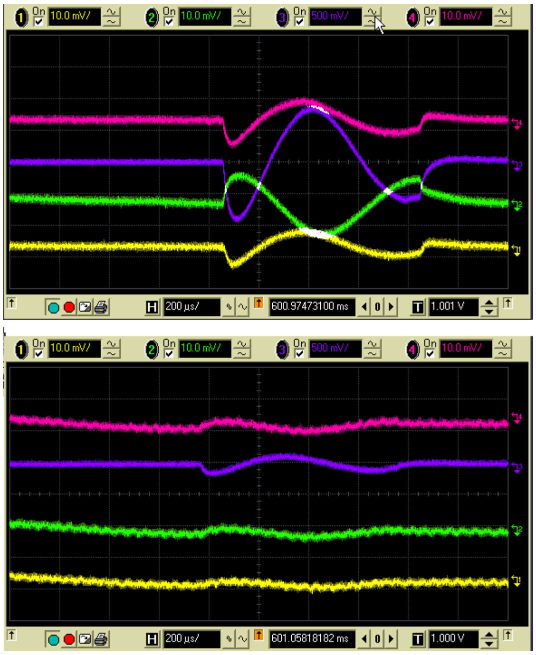

Figure 4: Noise observed on LTB FCT (green), BO FCT (yellow), BTS FCT1 upstream (pink) and BTS FCT2 downstream (purple) with booster extraction septum and pre-septum ON, before (top) and after (bottom) the noise improvement.

vacuum vessel (see Figure 5). This was because the end of the magnet winding was terminated to the earthed vacuum vessel, which served as its return path. The system was improved by removing the vacuum vessel termination and providing a low impedance direct return path with a single connection to earth.

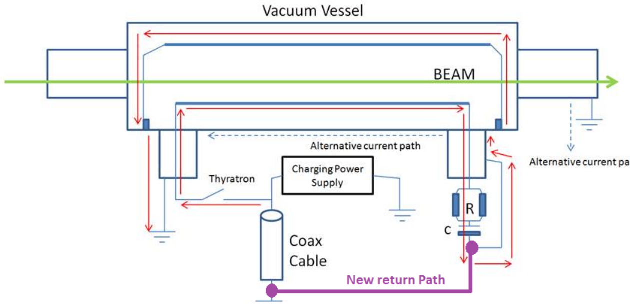

Figure 5: Return currents observed on the extraction kicker. The red arrows show the designed return path while the dashed blue arrows show the alternative current path that was creating noise to the system. The thick purple line shows the return path after the improvements.

The shielding of the kicker power supply enclosure was improved, too. The original meshed cage was replaced by a fully closed, 3 mm thick alodine finished aluminium box, and RF gaskets were added on all openings (see Figure 6).

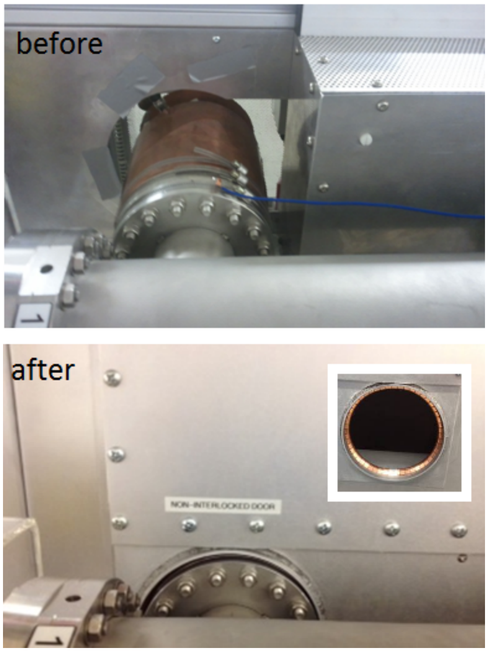

Figure 6: Kicker enclosure before (top) and after (bottom) the improvements. The insert in the bottom photo show the RF gaskets.

The improvements resulted in a 60% peak-to-peak noise reduction. As most of the disturbances were radiated noise, noise reduction could only be observed once the shielding was installed.

### *Background Subtraction*

Despite the large improvement that followed the earthing of the kicker background subtraction is recommended to let the acquisition cards integrate the cleanest possible data.

To perform the background subtraction all the magnets of the machine are powered up and triggered at 1 Hz by the injection or extraction trigger, but the gun is not fired. The noise coming from various magnets can then be observed, saved as PVs and were shown to have a consistent shape over the period of a one week top-up run. The background PVs are subtracted from the monitors' data PVs taken during user beam.

A new background is recorded at the beginning of every top-up run, i.e. about every week.

The background data of the monitors, their signal after background subtraction and their integrated charge is available at each injection through a graphical user interface (see Figure 7).

## INJECTION EFFICIENCY INTERLOCK

To maintain low radiation doses around the facility an interlock has been placed on the injection efficiency value measured between the last FCT in the BTS (BTS FCT2) and the delta current measurement of the SR DCCT. This interlock is software based and is currently set at 20 %. It is expected that the settings of the SR scrapers decrease the injection efficiency. When 2 consecutive injection shots

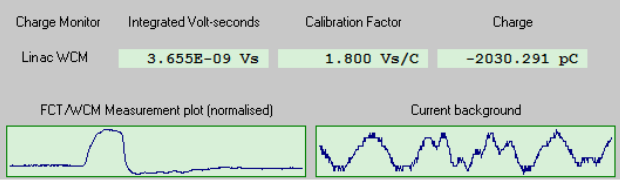

| Charge Monitor | Integrated Volt-seconds | Calibration Factor | Charge |
|---|---|---|---|
| Linac WCM | 3.655E-09 Vs | 1.800 Vs/C | -2030.291 pC |

Figure 7: Background (right), signal after background subtraction (left) and calculated charge (top) of the WCM during one injection.

have an efficiency lower than the limit the operation mode is reversed to decay mode.

As the DCCTs and FCTs PVs are located on two different IOCs, the BTS FCT2 to SR DCCT injection efficiency is calculated as follows:

The charge of BTS FCT2 is recorded 150 ms before the second measurement of the SR DCCT current. Once the FCT charge is determined its value is accessed by the original system IOC. The SR DCCT current is then measured. The value of the delta current calculated and then converted into charge. The coefficient of proportionality between SR DCCT current and charge is equal to the Storage Ring Orbit Clock [3], i.e. the revolution frequency of electrons in the SR. The injection efficiency is the ratio of the charges of both monitors.

## USER INTERFACE

The injection efficiency can be monitored on the graphical user interface (GUI), see Figure 8, which displays the efficiencies of last 70 injections for consecutive monitors. One observes that the booster injection to extraction efficiency is ≈ 65%. Major losses are known to happen in the first BO turn. To minimise the losses the booster ramp will be reviewed in the future. For this purpose the booster beam position monitors have been upgraded [4].

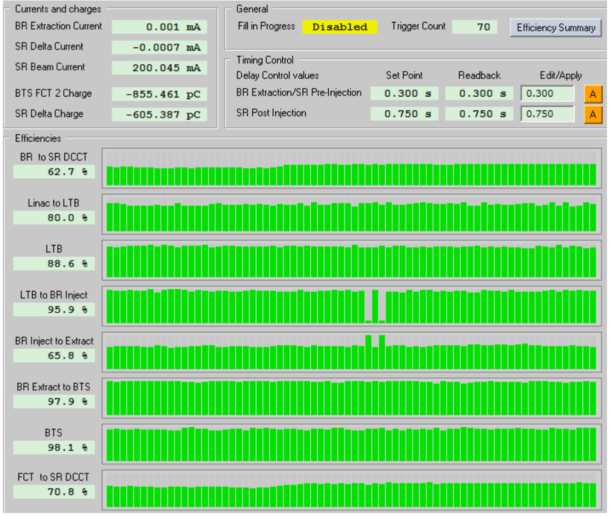

Currents and charges

| | |
|---|---|
| BR Extraction Current | 0.001 mA |
| SR Delta Current | -0.0007 mA |
| SR Beam Current | 200.045 mA |
| BTS FCT 2 Charge | -855.461 pC |
| SR Delta Charge | -605.387 pC |

General

Fill in Progress: Disabled
Trigger Count: 70

Timing Control

| Delay Control values | Set Point | Readback | Edit/Apply |
|---|---|---|---|
| BR Extraction/SR Pre-Injection | 0.300 s | 0.300 s | 0.300 |
| SR Post Injection | 0.750 s | 0.750 s | 0.750 |

Efficiencies

| | |
|---|---|
| BR to SR DCCT | 62.7 % |
| Linac to LTB | 80.0 % |
| LTB | 88.6 % |
| LTB to BR Inject | 95.9 % |
| BR Inject to Extract | 65.8 % |
| BR Extract to BTS | 97.9 % |
| BTS | 98.1 % |
| FCT to SR DCCT | 70.8 % |

Figure 8: GUI showing the last 70 efficiencies.

## CONCLUSION

In order to monitor the injection efficiency along the whole injection system and minimise radiation dose the injection efficiency monitoring system has been upgraded. It allows for the monitoring of the current at eight locations along the machine, and the calculation of intermediate efficiencies, from the electron gun to the Storage Ring. For safety an interlock that prevents the gun from firing has been placed on the value of the efficiency from the end of the BTS to the SR. This reliable monitoring system is in use during user beam. It will help to monitor and improve the user top-up operation into the future.

## REFERENCES

[1] E. van Garderen, et al., "Newly installed beam diagnostics at the Australian Synchrotron", DIPAC11, Hamburg, 2011, MOPD07

[2] A. Cole, et al., "Injection efficiency monitor at the Australian Synchrotron", EPJ web of conferences **35**, 2012

[3] E. van Garderen, et al., "Upgrade of the timing system at the Australian Synchrotron", DIPAC09, Basel, 2009, TUPD27

[4] E. van Garderen, et al., "Upgrade of the booster beam position monitors at the Australian Synchrotron", IPAC10, Kyoto, 2010, MOPD080